Published in final edited form as:
Cancer Res. 2010 November 1; 70(21): 8948–8958. doi:10.1158/0008-5472.CAN-10-1936.

Cell Signaling by Urokinase-type Plasminogen Activator Receptor Induces Stem Cell–like Properties in Breast Cancer Cells

Minji Jo[1], **Boryana M. Eastman**[1], **Drue L. Webb**, **Konstantin Stoletov**, **Richard Klemke**, and **Steven L. Gonias**[2]
Department of Pathology and the Moores Cancer Center, University of California San Diego, La Jolla, CA, USA

Abstract

Signaling by urokinase-type plasminogen activator receptor (uPAR) can cause epithelial-mesenchymal transition (EMT) in cultured breast cancer cells. In this report, we show that uPAR signaling can also induce cancer stem cell (CSC)-like properties. Ectopic overexpression of uPAR in human MDA-MB-468 breast cancer cells promoted emergence of a CD24-/CD44+ phenotype, characteristic of CSCs, while increasing the cell surface abundance of integrin subunits β1/CD29 and α6/CD49f that represent putative mammary gland stem cell biomarkers. uPAR overexpression increased mammosphere formation in vitro and tumor formation in an immunocompromised SCID mouse model of orthotopic breast cancer. Hypoxic conditions that are known to induce EMT in MDA-MB-468 cells also increased cell surface β1/CD29, mimicking the effects of uPAR overexpression. Antagonizing uPAR effector signaling pathways reversed the increase in cell surface integrin expression. While uPAR overexpression did not induce EMT in MCF-7 breast cancer cells, CSC-like properties were nevertheless still induced along with an increase in tumor initiation and growth in the orthotopic setting in SCID mice. Notably, in MCF-7 cell mammospheres, which display a well-defined acinus-like structure with polarized expression of E-cadherin and β1-integrin, cell collapse into the central cavity was decreased by uPAR overexpression, suggesting that uPAR signaling may stabilize epithelial morphology. In summary, our findings demonstrate that uPAR signaling can induce CSC-like properties in breast cancer cells, either concomitantly with or separately from EMT.

Keywords

urokinase-type plasminogen activator; uPAR; epithelial-mesenchymal transition; cancer stem cell; integrin; cell-signaling

Introduction

The epithelium of the normal mammary gland includes basal and luminal cells. Stem cells are present principally within the basal layer and responsible for normal mammary gland development and regeneration (1). Normal mammary gland stem cells (MGSCs) express high levels of the integrins: β1/CD29 and α6/CD49f (1–3), which serve not only as MGSC markers but also may play a functional role in stem cell behavior, reflecting their activity in cell adhesion and cell-signaling (4–5).

[2]**Corresponding Author:** Steven L. Gonias, UCSD School of Medicine, Department of Pathology, 9500 Gilman Drive, La Jolla California, 92093. Phone - 858-534-1887; Fax - 858-534-0414; sgonias@ucsd.edu.
[1]These authors contributed equally

According to the cancer stem cell (CSC) hypothesis, a subset of tumor cells may be responsible for development and progression of leukemia, lymphoma, and solid malignancies (6–8). CSCs demonstrate the capacity for self-renewal and the ability to generate daughter cells, which differentiate into the various morphologies and phenotypes observed in the mature cancer. How best to recognize a CSC within a complex tumor cell population remains a topic of intense investigation; however, in breast cancer, CSCs are frequently identified by a $CD44^{high}/CD24^{low}$ phenotype using flow cytometry (9). Integrin subunits, which are expressed in normal MGSCs, also may be important in breast CSCs (10–11).

Considerable evidence has emerged suggesting that the cell-signaling and transcription regulatory pathways that induce epithelial-mesenchymal transition (EMT) in carcinoma cells overlap with those activated in CSCs (12–13). The urokinase-type plasminogen activator (uPA) receptor (uPAR) induces EMT in cancer cells by activating diverse cell-signaling pathways, including the Ras-ERK pathway, the PI3K-Akt pathway, and Rac1 (14–15). Because uPAR expression is increased in hypoxia, uPAR-induced EMT may be important in large, poorly vascularized tumors. uPAR-induced EMT is reversible. Strategies that have been successfully used to reverse uPAR-induced cancer cell EMT include re-oxygenation, blocking uPA-binding to uPAR, and targeting cell-signaling pathways downstream of uPAR (14).

uPAR is a glycosyl phosphatidylinositiol-anchored receptor (16). Its activity in cell-signaling requires integrin co-receptors, such as $\alpha_4\beta_1$ and $\alpha_5\beta_1$ (17–19). Receptor tyrosine kinases, such as the EGFR, also may be engaged in uPAR-dependent cell-signaling (20–21). It is well known that many cancers demonstrate an increased propensity for metastasis in humans when uPAR expression is high (22). This may be explained by the effects of uPAR on cell-signaling, its ability to promote activation of proteases near the leading edge of cell migration, the function of uPAR as a vitronectin adhesion receptor, or its more recently described role in EMT (16, 23–25). Although the ability of uPAR to promote protease activation near the cell surface has been studied most exhaustively, at least in mice, uPAR promotes cancer progression by protease-independent mechanisms (26).

In this study, we demonstrate that breast cancer cells acquire robust CSC-like properties when uPAR is over-expressed and uPAR-dependent cell-signaling is activated. In MDA-MB-468 cells, acquisition of CSC-like properties is associated with EMT; however, in MCF-7 cells, CSC-like properties develop independently of EMT. The difference may reflect availability of uPA, which is important to activate some cell-signaling pathways downstream of uPAR, and other receptor systems, which control the physiology of these cells.

Materials and Methods

Reagents

Anti-CD24-fluorescein isothiocyanate (FITC) (ML5), anti-CD44-phycoerythrin (PE) (G44-26), and isotype-matched IgGs were from BD Biosciences. Anti-CD29-FITC (HMβ1-1) and anti-CD49f-PE (GoH3) were from Biolegend. Rat monoclonal antibody that recognizes β1 integrin (AIIB2) was from the Developmental Studies Hybridoma Bank (University of Iowa). Monoclonal antibody that detects activated β1 integrin (HUTS4) was from Millipore. Monoclonal human uPAR-specific antibody (ATN658) and polyclonal human uPAR-specific anti-sera were provided by Dr. Andrew Mazar. E-cadherin-specific monoclonal antibody HECD-1 and polyclonal α6 integrin-specific antibody were from Abcam. Monoclonal antibody that recognizes vimentin was from Sigma-Aldrich. Secondary antibodies conjugated with AlexaFluor 488, AlexaFluor 569 and AlexaFluor 647 were from Invitrogen. PI3K inhibitor (LY294002) and MEK1 inhibitor (PD098059) were from EMD Biosciences. B27 serum-free supplement was from Invitrogen. bFGF and EGF were from R&D systems. qPCR reagents,

including primers and probes for human uPAR and HPRT-1, were from Applied Biosystems. Primer sets for β1 integrin were synthesized by Integrated DNA Technologies.

Cell culture

Human uPAR over-expressing MDA-MB-468 cells (468/uPAR) and empty vector-transfected MDA-MB-468 cells (468/EV) are previously described (15). MCF-7 cells that over-express human uPAR (MCF-7/uPAR) were prepared by transfecting cells with pcDNA-uPAR using Lipofectamine 2000. After selection for 14 days with 500 μg/ml hygromycin, single-cell clones were established and screened for uPAR expression by immunoblot analysis. The cells were maintained in DMEM (HyClone) supplemented with 10% FBS, 100 U/ml penicillin, and 100 μg/ml streptomycin.

Flow cytometry

Cells (3×10^6) were plated in 10-cm dishes and in some studies, treated with LY294002 (10 μM) or PD098059 (50 μM) in serum-free medium for 18 h. Cells were re-suspended in FACS buffer (2% BSA in PBS) and incubated with anti-CD29-FITC (0.5 μg/10^6 cells), anti-CD49f-PE (10 μl/test), anti-CD24-FITC (10 μl/test), anti-CD44-PE (10 μl/test), or isotype-matched IgG for 30 min on ice. To detect uPAR or activated β1 integrin, cells were incubated with primary antibodies (1 μg/10^6 cells) for 1 h. Primary antibodies were detected using secondary antibodies conjugated with AlexaFluor 488 or AlexaFluor 647. Results were analyzed using a FACSCanto II (BD Biosciences) and FlowJo software.

Biotinylation of cell-surface proteins

Cells in monolayer culture (1.5×10^6) were washed three times with ice-cold PBS and then treated with EZ-link sulfo-NHS-SS-biotin (1 mg/ml, Pierce) for 15 min on ice. Biotinylation reactions were terminated with 100 mM glycine in PBS. After washing with PBS, cell extracts were prepared in RIPA buffer (20 mM sodium phosphate, 150 mM NaCl, pH 7.4, 1% NP-40, 0.1% SDS, and 0.5% deoxycholic acid) with protease inhibitor cocktail (Roche). Biotinylated membrane proteins were precipitated with Streptavidin-Sepharose (GE Healthcare). Proteins were eluted with SDS sample buffer, resolved by SDS-PAGE, electro-transferred to PVDF membranes and probed with primary antibodies.

Immunoblot analysis

Cell extracts were prepared in RIPA buffer containing complete protease inhibitor cocktail. Protein concentrations were determined by bicinchoninic acid assay (Sigma-Aldrich). Equal amounts of cell extract were resolved by SDS-PAGE, electro-transferred to PVDF membranes, and probed with primary antibodies.

Mammosphere assay

Cells were trypsinized and mechanically disrupted to obtain single cell suspensions. The cells were then cultured in mammosphere medium (DMEM/F12, B27, 20 ng/mL bFGF, 20 ng/mL EGF, 100 U/ml penicillin and 100 μg/ml streptomycin) in ultra-low attachment 24-well plates (Corning) at a density of 2,000, 500 or 50 cells/500 μL for 7–10 days. Mammospheres were imaged and counted under phase-contrast microscopy. Only mammospheres exceeding 100 μm in diameter were counted.

As a second assay to assess mammosphere formation, cultures were established in ultra-low attachment 96-well plates as a density of one cell/well. Mammosphere formation was assessed after culturing for 7–10 days. This second method assured that mammospheres were formed by a single cell.

Tumor formation assay

Animal experimentation was done in accordance with protocols approved by the University of California San Diego Animal Care Program. Anesthetized 8 week-old C.B-17/lcrCrl-scid-BR mice (Charles River Laboratories) were inoculated in the fourth and contralateral fourth mammary fat pads with 50, 100 or 1000 468/EV or 468/uPAR cells suspended in 50 μL of Matrigel (Sigma). MCF-7/EV or MCF-7/ uPAR cells also were injected into mammary fat pads (1×10^6 cells/injection). Primary tumor growth was monitored every 2 to 3 days. One month after injection of MDA-MB-468 cells or 10 weeks after injection of MCF-7 cells, mice were euthanized and the mammary fat pads were visually inspected for tumor. Tumor formation was confirmed by histological analysis. Data processing and statistical analysis were performed using GraphPad Prism (GraphPad Software, Inc.) and Microsoft Excel (Microsoft Corporation).

Histology and immunohistochemistry

Formalin-fixed tissue was paraffin-embedded. Serial 4 μm sections were stained with hematoxylin and eosin. Immunohistochemistry was performed using the Vantana Discovery® XT System (Vantana). Sections were pretreated with citric acid buffer and then incubated with polyclonal antibody specific for human uPAR (1:200) followed by peroxidase-conjugated secondary antibody. Peroxidase activity was imaged using 3,3'-diaminobenzidine. Slides were examined using a Leica DM2500 light microscope. Images were acquired using a Leica DFC420 digital camera and Leica Application Suite software.

qPCR analysis

Total RNA was isolated using the RNeasy kit (Qiagen). cDNA was synthesized using the iScript kit (BioRad). qPCR was performed using an Applied Biosystems instrument and a one-step program: 95°C, 10 min; 95°C, 30 s and 60°C, 1 min for 40 cycles. HPRT-1 gene expression was measured as a normalizer. Results were analyzed by the relative quantity (ΔΔCt) method. All experiments were performed in triplicate with internal duplicate determinations.

Cell adhesion assays

Medium-binding 96-well plates (Corning) were coated with fibronectin (5 μg/mL) or type I collagen (5 μg/mL) for 18 h at 4° C and then blocked with 1% (w/v) BSA for 2 h. Cells were washed and re-suspended in serum-free DMEM at a concentration of 0.5×10^6 cells/ml and allowed to adhere for 15 min at 37° C. Adherent cells were fixed with 4% formaldehyde and stained with crystal violet. The dye was eluted with 10% acidic acid and absorbance at 570 nm was determined. Each value represents the mean of 18 replicates in three separate experiments.

Immunofluorescence microscopy

Cells were plated on glass coverslips, fixed in 4% formaldehyde, permeabilized in 0.2% Triton X-100, and incubated with antibodies specific for e-cadherin (1:100) or vimentin (1:400) followed by secondary antibodies conjugated with AlexaFluor 488 or AlexaFluor 594. Preparations were mounted on slides using Pro-long Gold with DAPI (Invitrogen) and examined using a Leica DMIRE2 fluorescence microscope. Images were obtained using a 63x oil-immersion objective and a Hamamatsu digital camera with SimplePCI software.

Mammospheres were allowed to form in ultra-low attachment T25 flasks. The mammospheres were collected by centrifugation at 200 × g, suspended, fixed in 4% formaldehyde, permeabilized with 0.2% Triton X-100, and incubated with antibodies specific for β1 integrin (AIIB2, 1 μg/100 μL) and e-cadherin. Secondary antibodies were conjugated with AlexaFluor 488 or AlexaFluor 594. Control preparations were treated equivalently except for the omission

of primary antibody. Stained mammospheres were mounted on chamber slides using ProLong Gold (Invitrogen) and examined using a spectral confocal microscope (C1-si, Nikon).

Results

uPAR over-expressing MDA-MB-468 cells acquire CSC-like properties

Hypoxia increases uPAR expression, activates uPAR-dependent cell-signaling, and induces EMT in MDA-MB-468 breast cancer cells (15). Equivalent changes in cell phenotype are observed when uPAR is over-expressed. Because others have suggested that the cell-signaling pathways responsible for EMT in cancer cells overlap with those activated in CSCs (13), we tested whether uPAR-over-expression in MDA-MB-468 cells induces CSC-like properties. Fig. 1A shows that the abundance of cell-surface uPAR was substantially increased in uPAR over-expressing (468/uPAR) cells. Although the level of CD44 was already high in control (468/EV) cells, a subpopulation of the cells shifted to a higher level of CD44 expression when uPAR was over-expressed. CD24 was significantly decreased in the majority of the 468/uPAR cells (Fig. 1B).

Next, we examined whether uPAR over-expression alters the abundance of cell-surface integrins that have been described as mammary gland stem cell biomarkers. Total β1/CD29 was substantially increased at the cell surface in 468/uPAR cells, as was activated β1, as determined with antibody HUTS4. α6/CD49f also was increased, although the increase observed by flow cytometry was less pronounced than that observed for β1/CD29 (Fig. 1C). To confirm that cell-surface α6/CD49f is regulated in 468/uPAR cells, we biotinylated cell-surface proteins for isolation by affinity precipitation. Fig. 1D shows that cell-surface α6/CD49f was increased in 468/uPAR cells, whereas the total level of α6/CD49f was unchanged.

468/uPAR and 468/EV cells formed mammospheres in suspension culture, providing evidence that cells with self renewal capacity were present (Fig. 1E). The mammospheres did not demonstrate a well organized structure, compared with those formed by MCF-7 cells (see below). Nevertheless, the number of mammospheres formed by 468/uPAR cells was significantly increased ($p<0.01$), compared with the number formed by 468/EV cells (Fig. 1F). The ability of uPAR over-expression to promote mammosphere formation was demonstrated in different studies in which suspension cultures were established at varied density. To confirm that mammospheres formed from a single cell, single-cell cultures of 468/uPAR cells and 468/EV cells were established in ultra-low attachment 96-well plates. Fig. 1G shows that the percentage of cultures that generated a mammosphere was significantly increased when uPAR was over-expressed (n=4, $p<0.01$).

To test whether uPAR over-expression promotes tumor initiation by MDA-MB-468 cells *in vivo*, we performed limiting dilution assays, injecting 1,000, 100, or 50 cells into mammary fat pads in SCID mice. As shown in Table 1, when 1,000 or 100 cells were injected, 468/uPAR and 468/EV cells formed tumors equivalently. However, when 50 cells were injected, 468/uPAR cells formed tumors at a significantly increased rate ($p<0.05$). The results of our flow cytometry experiments, mammosphere assays, and limiting dilution studies support a model in which uPAR over-expression engenders CSC-like properties in MDA-MB-468 cells.

uPAR-initiated cell-signaling regulates the subcellular distribution of β1 integrin

Because MDA-MB-468 cells express uPA endogenously, over-expression of uPAR results in activation of PI3K and ERK/MAP kinase (15). uPAR also physically associates with integrins in the plasma membrane (17). Either of these non-mutually exclusive mechanisms could be responsible for the increase in cell-surface β1 integrin observed in 468/uPAR cells. To test whether cell-signaling is involved, 468/uPAR cells were treated with the MEK inhibitor,

PD098059 (50 μM), or with the PI3K inhibitor, LY294002 (10 μM). In three separate experiments, both reagents significantly decreased the level of cell-surface β1/CD29, α6/CD49f, and activated β1/CD29, as determined with antibody HUTS4 (Fig. 2).

As a second model system to study cells in which increased uPAR expression drives EMT, we exposed MDA-MB-468 cells to 1.0% O_2 for 48 h. Fig. 3A shows that uPAR mRNA expression increased 3-fold, confirming our previous results (15). β1 integrin subunit mRNA was unchanged. The cell-surface abundance of β1 integrin was examined by biotinylation and affinity precipitation. Fig. 3B shows that cell-surface β1 integrin was substantially increased in MDA-MB-468 cells that were exposed to hypoxia. β1 integrin in whole cell extracts distributed into two bands; the mature form found at the cell-surface, which is more slowly migrating, and the more rapidly migrating immature form. Although the total level of β1 integrin (sum of two bands) did not change significantly in hypoxia, the distribution of β1 integrin between the two bands shifted so that more mature β1 integrin was present. This result confirms our affinity precipitation data, demonstrating that hypoxia increases the abundance of cell-surface β1 integrin.

uPAR over-expression induces CSC-like properties independently of EMT in MCF-7 breast cancer cells

uPAR over-expression does not induce EMT uniformly in all cancer cells (15). The degree to which the cancer cells express uPA endogenously and the function of other receptors that regulate cancer cell physiology may be involved. MCF-7 cells are estrogen receptor-positive breast cancer cells that express low levels of uPAR and undetectable uPA (24). We over-expressed uPAR in MCF-7 cells and isolated two single-cell clones (C4 and C5). uPAR over-expression was confirmed by flow cytometry (Fig. 4A). Neither of the uPAR-over-expressing MCF-7 cell clones demonstrated signs of EMT. Fig. 4B shows the results of experiments performed with C5 cells, which expressed the highest level of cell-surface uPAR. Compared with cells that were transfected with empty vector (MCF-7/EV), C5 MCF-7/uPAR cells demonstrated an unchanged level of e-cadherin and no vimentin. By contrast, 468/uPAR cells demonstrated a substantial decrease in e-cadherin and high levels of vimentin, as previously demonstrated (15). These results were confirmed by immunoflourescence microscopy (Fig. 4C). Note the robust vimentin immunopositivity in uPAR-over-expressing MDA-MB-468 cells. uPAR-over-expressing MCF-7 cells retained e-cadherin at cell-cell junctions, while vimentin was not detected.

To determine whether uPAR over-expression induces CSC-like properties in MCF-7 cells, C4 and C5 MCF-7/uPAR cells were analyzed by flow cytometry (Fig. 5A). CD24 expression was decreased in the majority of the C4 and C5 MCF-7/uPAR cells, compared with MCF-7/EV cells. Again, as is frequently the case in cancer cell lines, CD44 was already expressed at high levels in the control cells; uPAR over-expression slightly decreased CD44 in the C5 clone. However, both β1/CD29 and α6/CD49f were increased in the C4 and C5 MCF-7/uPAR cells.

Because the increase in cell-surface integrin expression induced by uPAR overexpression in MCF-7 cells was less robust than that observed in 468/uPAR cells, we performed cell adhesion assays to a test whether integrin function was regulated. Adhesion of C5 MCF-7/uPAR cells and control MCF-7/EV cells to the β1 integrin ligands, type 1 collagen and fibronectin, was compared. Fig. 5B shows that adhesion of C5 cells to both substrata was significantly increased ($p<0.01$).

Mammosphere assays were performed to compare the self-renewal activity of C5 MCF-7/uPAR and MCF-7/EV cells. Mammospheres formed by MCF-7 cells showed substantial differentiation into spheroid-like structures (Fig. 5C). Regularly contoured external borders and partially hollow central cavities were observed. As shown in Fig. 5D, uPAR over-

expression in MCF-7 cells increased the frequency of mammosphere formation 4–5-fold irrespective of the number of cells that were introduced into each well ($p<0.05$ at each density). In experiments with single-cell cultures, uPAR-over-expression increased mammosphere formation 3-fold ($p<0.05$), confirming the results shown in Fig. 5D (results not shown).

Non-malignant mammary epithelial cells, such as MCF10A cells, form polarized, acinus-like spheroids in three-dimensional culture, recapitulating the grandular structure of normal mammary glands (27). In the acinus-like structures, β1 integrin is localized basally and e-cadherin to cell junctions. Fig. 6A shows that in mammospheres formed by MCF-7 cells, β1 integrin polarized principally to the inner surface of the central cavity. Some β1 integrin also was detected at cell junctions, reminiscent of normal mammary gland structure *in vivo* (3,28). E-cadherin localized to cell-cell junctions and also, to some extent, to the inner surface of the central cavities, co-localizing with β1 integrin. In the control MCF-7/EV cells, the inner cavities of most mammospheres were partially collapsed by cells growing inward. By contrast, in mammospheres formed by uPAR-over-expressing MCF-7 cells, collapse of cells into the central cavity was much less frequent. As a result, these mammospheres more rigorously approximated a normal mammary gland acinus-like structure. The distribution of β1 integrin and e-cadherin in mammospheres formed by C5 MCF-7/uPAR cells was similar to that observed in MCF-7/EV cells. These studies confirm that in MCF-7 cells, CSC-like properties are induced by uPAR-over-expression independently of signs of EMT.

uPAR over-expression in MCF-7 cells promotes tumor initiation *in vivo*

In the absence of estrogen supplementation, orthotopic tumor formation by MCF-7 cells in SCID mice is limited even when a large number of cells is injected (29). As shown in Table 2 (see supplementary data), uPAR over-expression significantly increased the frequency of tumor formation from equivalently-sized inoculums ($p<0.05$). Tumors formed by uPAR-over-expressing cells grew much larger in the timeframe of the study (Fig. 6B); the mean volume of the tumor was increased more than 20-fold. The malignant cells within the tumors remained robustly uPAR-immunopositive *in vivo*, as determined by immunohistochemistry (Fig. 6C). Non-malignant mouse cells that infiltrated the tumor were immunonegative for uPAR, as determined with our human uPAR-specific antibody.

Discussion

In diverse human malignancies, high levels of uPAR expression are associated with an increased propensity for cancer progression and metastasis (22,30). Studies analyzing uPAR at the cellular and molecular level have revealed multiple candidate mechanisms. The ability of uPAR to accelerate a number of extracellular reactions, including conversion of the zymogen form of uPA into the active two-chain form (tcuPA) (31) and plasminogen activation by tcuPA (32), promotes proteolysis and remodeling of the extracellular matrix (ECM). Because uPAR polarizes to the leading edge of cellular migration (33), increased ECM remodeling may facilitate cancer cell migration and invasion through tissue boundaries.

uPAR also may promote cancer progression by its effects on cell adhesion and cell-signaling. The importance of this mechanism is supported by recent mouse model experiments (26). In addition to uPA, uPAR functions as a receptor for the ECM protein, vitronectin (25). Binding of uPA or vitronectin to uPAR activates distinct cell-signaling pathways, which collectively support cell migration and survival (23–24,26,34–36). Understanding how uPAR-dependent cell-signaling regulates cancer cell physiology is an important goal. In some cancer cell lines, increased uPAR expression and activation of uPAR-dependent cell-signaling in hypoxia induce EMT (15). Our evidence suggests that the full continuum of uPAR-initiated cell-signaling pathways, including those activated downstream of uPA and vitronectin, may be

necessary for EMT (14,15). However, the factors that control whether uPAR induces EMT remain incompletely understood.

In this study, we demonstrated that uPAR over-expression does not induce EMT in MCF-7 cells. In fact, the polarized epithelial morphology of these cells may be strengthened by uPAR, since collapse of cells into central cavities of mammospheres was decreased. Whether EMT occurs in human cancer *in vivo* and thus represents a relevant pathway affecting cancer progression remains unsettled (37). Hypoxia-induced EMT, under the control of uPAR, is reversible (14). Thus, the fact that metastases in organs such as the lungs frequently demonstrate well-defined epithelial morphology does not preclude that EMT occurred as a step in the metastasis cascade.

In a cell type that undergoes uPAR-induced EMT (MDA-MB-468) and in a cell type that does not (MCF-7), uPAR-over-expression engendered cells with biomarkers and properties of CSCs. In MDA-MB-468 cells, uPAR over-expression significantly increased the likelihood of tumor initiation by a small number of cancer cells *in vivo*. uPAR over-expression was associated with a $CD44^{high}/CD24^{low}$ phenotype, increased cell-surface β1/CD29 and α6/CD49f, and a significant increase in mammosphere formation frequency. Thus, in this cell type, the correlation between EMT and CSC-like properties was upheld. In MCF-7 cells, CSC-like properties associated with uPAR overexpression included decreased CD24 expression, an increase in the cell surface abundance of β1/CD29 and α6/CD49f, and an increased frequency of mammosphere formation. Although the requirement for estrogen supplementation *in vivo* precluded typical serial dilution studies with MCF-7 cells, we did demonstrate that uPAR over-expression significantly increases the frequency of tumor initiation and tumor growth in SCID mice. We previously demonstrated that uPAR-induced EMT is reversible (14). Because the signaling pathways downstream of uPAR that are responsible for EMT and CSC-like properties may be at least partially overlapping, it is possible that uPAR-induced CSC-like properties also may be dynamic and reversible.

MDA-MB-468 cell mammospheres demonstrated poorly defined structure consistent with the loss of epithelial morphology and EMT. By contrast, mammospheres formed by MCF-7 cells showed a highly ordered and polarized structure with β1 integrin localized principally to a single surface and E-cadherin at cell-cell junctions. Interestingly, the β1 integrin subunit localized mainly to the internal surface of the mammosphere, opposite the location in a normal mammary acinus or duct. MCF-7 cells are frequently thought to have arisen from luminal epithelium (38). The increase in expression of cell-surface β1 integrin, which accompanies uPAR over-expression, may indicate a transformation to a more basal cell phenotype.

In response to uPAR over-expression or hypoxia, β1 integrin in MDA-MB-468 cells relocated to the cell surface from intracellular pools. It is well established that uPAR associates with integrins in the plasma membrane (17–18,39–41) and that integrins function as co-receptors in uPAR-initiated cell-signaling (17,23,41–42). Receptors other than uPAR, which activate similar signal transduction pathways, also may cause relocation of β1 integrin to the cell surface (43). This process may provide a positive feedback loop by which uPAR-initiated cell-signaling is strengthened.

When the cell surface abundance of uPAR was increased, the level of activated β1 integrin was increased, as determined with antibody HUTS4. Integrins exist in conformations that favor ligand-binding or not; fluctuation between these conformational states may be controlled by cell-signaling pathways (44), many of which are controlled downstream of uPAR (23,45). Thus, it is not surprising that HUTS4 reactivity in uPAR-over-expressing MDA-MB-468 cells was decreased by inhibitors of PI3K and ERK/MAP kinase activation. However, these results do not rule out the possibility that uPAR also regulates integrin conformation by cis-

interactions within the plasma membrane. Regulation of integrin activation by uPAR represents another possible positive feedback pathway by which uPAR and integrins may cooperate to control cancer cell physiology.

For the most part, uPAR has been studied as a gene product that controls invasion and metastasis of existing cancers. The function of uPAR as a gene product involved in generating CSC-like properties re-focuses attention on this receptor to earlier steps in cancer development. In normal human adults, uPAR is sparsely expressed in tissues and organs (22). Thus, uPAR could serve as a target for cancer diagnostics development or therapeutics aimed at early stages of cancer.

Supplementary Material

Refer to Web version on PubMed Central for supplementary material.

Acknowledgments

Grant support: NIH R01 CA94900

References

1. Stingl J, Eirew P, Ricketson I, et al. Purification and unique properties of mammary epithelial stem cells. Nature 2006;439:993–997. [PubMed: 16395311]
2. Shackleton M, Vaillant F, Simpson KJ, et al. Generation of a functional mammary gland from a single stem cell. Nature 2006;439:84–88. [PubMed: 16397499]
3. Taddei I, Deugnier MA, Faraldo MM, et al. Beta1 integrin deletion from the basal compartment of the mammary epithelium affects stem cells. Nat Cell Biol 2008;10:716–722. [PubMed: 18469806]
4. Pontier SM, Muller WJ. Integrins in mammary-stem-cell biology and breastcancer progression--a role in cancer stem cells? J Cell Sci 2009;122:207–214. [PubMed: 19118213]
5. Schwartz MA. Integrin signaling revisited. Trends Cell Biol 2001;11:466–470. [PubMed: 11719050]
6. Klonisch T, Wiechec E, Hombach-Klonisch S, et al. Cancer stem cell markers in common cancers - therapeutic implications. Trends Mol Med 2008;14:450–460. [PubMed: 18775674]
7. Stingl J, Caldas C. Molecular heterogeneity of breast carcinomas and the cancer stem cell hypothesis. Nat Rev Cancer 2007;7:791–799. [PubMed: 17851544]
8. Visvader JE, Lindeman GJ. Cancer stem cells in solid tumours: accumulating evidence and unresolved questions. Nat Rev Cancer 2008;8:755–768. [PubMed: 18784658]
9. Al-Hajj M, Wicha MS, Benito-Hernandez A, Morrison SJ, Clarke MF. Prospective identification of tumorigenic breast cancer cells. Proc Natl Acad Sci U S A 2003;100:3983–3988. [PubMed: 12629218]
10. Cariati M, Naderi A, Brown JP, et al. Alpha-6 integrin is necessary for the tumourigenicity of a stem cell-like subpopulation within the MCF7 breast cancer cell line. Int J Cancer 2008;122:298–304. [PubMed: 17935134]
11. White DE, Kurpios NA, Zuo D, et al. Targeted disruption of beta1-integrin in a transgenic mouse model of human breast cancer reveals an essential role in mammary tumor induction. Cancer Cell 2004;6:159–170. [PubMed: 15324699]
12. DiMeo TA, Anderson K, Phadke P, et al. A novel lung metastasis signature links Wnt signaling with cancer cell self-renewal and epithelial-mesenchymal transition in basal-like breast cancer. Cancer Res 2009;69:5364–5373. [PubMed: 19549913]
13. Mani SA, Guo W, Liao MJ, et al. The epithelial-mesenchymal transition generates cells with properties of stem cells. Cell 2008;133:704–715. [PubMed: 18485877]
14. Jo M, Lester RD, Montel V, et al. Reversibility of epithelial-mesenchymal transition (EMT) induced in breast cancer cells by activation of urokinase receptor-dependent cell signaling. J Biol Chem 2009;284:22825–22833. [PubMed: 19546228]
15. Lester RD, Jo M, Montel V, Takimoto S, Gonias SL. uPAR induces epithelial-mesenchymal transition in hypoxic breast cancer cells. J Cell Biol 2007;178:425–436. [PubMed: 17664334]

16. Blasi F, Carmeliet P. uPAR: a versatile signalling orchestrator. Nat Rev Mol Cell Biol 2002;3:932–943. [PubMed: 12461559]

17. Wei Y, Eble JA, Wang Z, Kreidberg JA, Chapman HA. Urokinase receptors promote beta1 integrin function through interactions with integrin alpha3beta1. Mol Biol Cell 2001;12:2975–2986. [PubMed: 11598185]

18. Wei Y, Lukashev M, Simon DI, et al. Regulation of integrin function by the urokinase receptor. Science 1996;273:1551–1555. [PubMed: 8703217]

19. Tarui T, Mazar AP, Cines DB, Takada Y. Urokinase-type plasminogen activator receptor (CD87) is a ligand for integrins and mediates cell-cell interaction. J Biol Chem 2001;276:3983–3990. [PubMed: 11053440]

20. Jo M, Thomas KS, O'Donnell DM, Gonias SL. Epidermal growth factor receptor-dependent and -independent cell-signaling pathways originating from the urokinase receptor. J Biol Chem 2003;278:1642–1646. [PubMed: 12426305]

21. Liu D, Aguirre Ghiso J, Estrada Y, Ossowski L. EGFR is a transducer of the urokinase receptor initiated signal that is required for in vivo growth of a human carcinoma. Cancer Cell 2002;1:445–457. [PubMed: 12124174]

22. Mazar AP. Urokinase plasminogen activator receptor choreographs multiple ligand interactions: implications for tumor progression and therapy. Clin Cancer Res 2008;14:5649–5655. [PubMed: 18794071]

23. Aguirre Ghiso JA, Kovalski K, Ossowski L. Tumor dormancy induced by downregulation of urokinase receptor in human carcinoma involves integrin and MAPK signaling. J Cell Biol 1999;147:89–104. [PubMed: 10508858]

24. Nguyen DH, Hussaini IM, Gonias SL. Binding of urokinase-type plasminogen activator to its receptor in MCF-7 cells activates extracellular signal-regulated kinase 1 and 2 which is required for increased cellular motility. J Biol Chem 1998;273:8502–8507. [PubMed: 9525964]

25. Wei Y, Waltz DA, Rao N, et al. Identification of the urokinase receptor as an adhesion receptor for vitronectin. J Biol Chem 1994;269:32380–32388. [PubMed: 7528215]

26. Jo M, Takimoto S, Montel V, Gonias SL. The urokinase receptor promotes cancer metastasis independently of urokinase-type plasminogen activator in mice. Am J Pathol 2009;175:190–200. [PubMed: 19497996]

27. Weaver VM, Petersen OW, Wang F, et al. Reversion of the malignant phenotype of human breast cells in three-dimensional culture and in vivo by integrin blocking antibodies. J Cell Biol 1997;137:231–245. [PubMed: 9105051]

28. Naylor MJ, Li N, Cheung J, et al. Ablation of beta1 integrin in mammary epithelium reveals a key role for integrin in glandular morphogenesis and differentiation. J Cell Biol 2005;171:717–728. [PubMed: 16301336]

29. Noel AC, Calle A, Emonard HP, et al. Invasion of reconstituted basement membrane matrix is not correlated to the malignant metastatic cell phenotype. Cancer Res 1991;51:405–414. [PubMed: 1988101]

30. de Bock CE, Wang Y. Clinical significance of urokinase-type plasminogen activator receptor (uPAR) expression in cancer. Med Res Rev 2004;24:13–39. [PubMed: 14595671]

31. Ellis V, Scully MF, Kakkar VV. Plasminogen activation initiated by single-chain urokinase-type plasminogen activator. Potentiation by U937 monocytes. J Biol Chem 1989;264:2185–2188. [PubMed: 2521625]

32. Ellis V, Behrendt N, Dano K. Plasminogen activation by receptor-bound urokinase. A kinetic study with both cell-associated and isolated receptor. J Biol Chem 1991;266:12752–12758. [PubMed: 1829461]

33. Estreicher A, Muhlhauser J, Carpentier JL, Orci L, Vassalli JD. The receptor for urokinase type plasminogen activator polarizes expression of the protease to the leading edge of migrating monocytes and promotes degradation of enzyme inhibitor complexes. J Cell Biol 1990;111:783–792. [PubMed: 2166055]

34. Jo M, Thomas KS, Marozkina N, et al. Dynamic assembly of the urokinase-type plasminogen activator signaling receptor complex determines the mitogenic activity of urokinase-type plasminogen activator. J Biol Chem 2005;280:17449–17457. [PubMed: 15728176]

35. Kjoller L, Hall A. Rac mediates cytoskeletal rearrangements and increased cell motility induced by urokinase-type plasminogen activator receptor binding to vitronectin. J Cell Biol 2001;152:1145–1157. [PubMed: 11257116]
36. Ma Z, Thomas KS, Webb DJ, et al. Regulation of Rac1 activation by the low density lipoprotein receptor-related protein. J Cell Biol 2002;159:1061–1070. [PubMed: 12499359]
37. Tarin D, Thompson EW, Newgreen DF. The fallacy of epithelial mesenchymal transition in neoplasia. Cancer Res 2005;65:5996–6000. discussion -1. [PubMed: 16024596]
38. Charafe-Jauffret E, Ginestier C, Monville F, et al. Gene expression profiling of breast cell lines identifies potential new basal markers. Oncogene 2006;25:2273–2284. [PubMed: 16288205]
39. Carriero MV, Del Vecchio S, Capozzoli M, et al. Urokinase receptor interacts with alpha(v)beta5 vitronectin receptor, promoting urokinase-dependent cell migration in breast cancer. Cancer Res 1999;59:5307–5314. [PubMed: 10537314]
40. Xue W, Mizukami I, Todd RF 3rd, Petty HR. Urokinase-type plasminogen activator receptors associate with beta1 and beta3 integrins of fibrosarcoma cells: dependence on extracellular matrix components. Cancer Res 1997;57:1682–1689. [PubMed: 9135008]
41. Yebra M, Parry GC, Stromblad S, et al. Requirement of receptor-bound urokinase-type plasminogen activator for integrin alphavbeta5-directed cell migration. J Biol Chem 1996;271:29393–29399. [PubMed: 8910604]
42. Nguyen DH, Catling AD, Webb DJ, et al. Myosin light chain kinase functions downstream of Ras/ERK to promote migration of urokinase-type plasminogen activator-stimulated cells in an integrin-selective manner. J Cell Biol 1999;146:149–164. [PubMed: 10402467]
43. Roberts MS, Woods AJ, Dale TC, Van Der Sluijs P, Norman JC. Protein kinase B/Akt acts via glycogen synthase kinase 3 to regulate recycling of alpha v beta 3 and alpha 5 beta 1 integrins. Mol Cell Biol 2004;24:1505–1515. [PubMed: 14749368]
44. Hynes RO. Integrins: bidirectional, allosteric signaling machines. Cell 2002;110:673–687. [PubMed: 12297042]
45. Monaghan-Benson E, McKeown-Longo PJ. Urokinase-type plasminogen activator receptor regulates a novel pathway of fibronectin matrix assembly requiring Src-dependent transactivation of epidermal growth factor receptor. J Biol Chem 2006;281:9450–9459. [PubMed: 16461772]

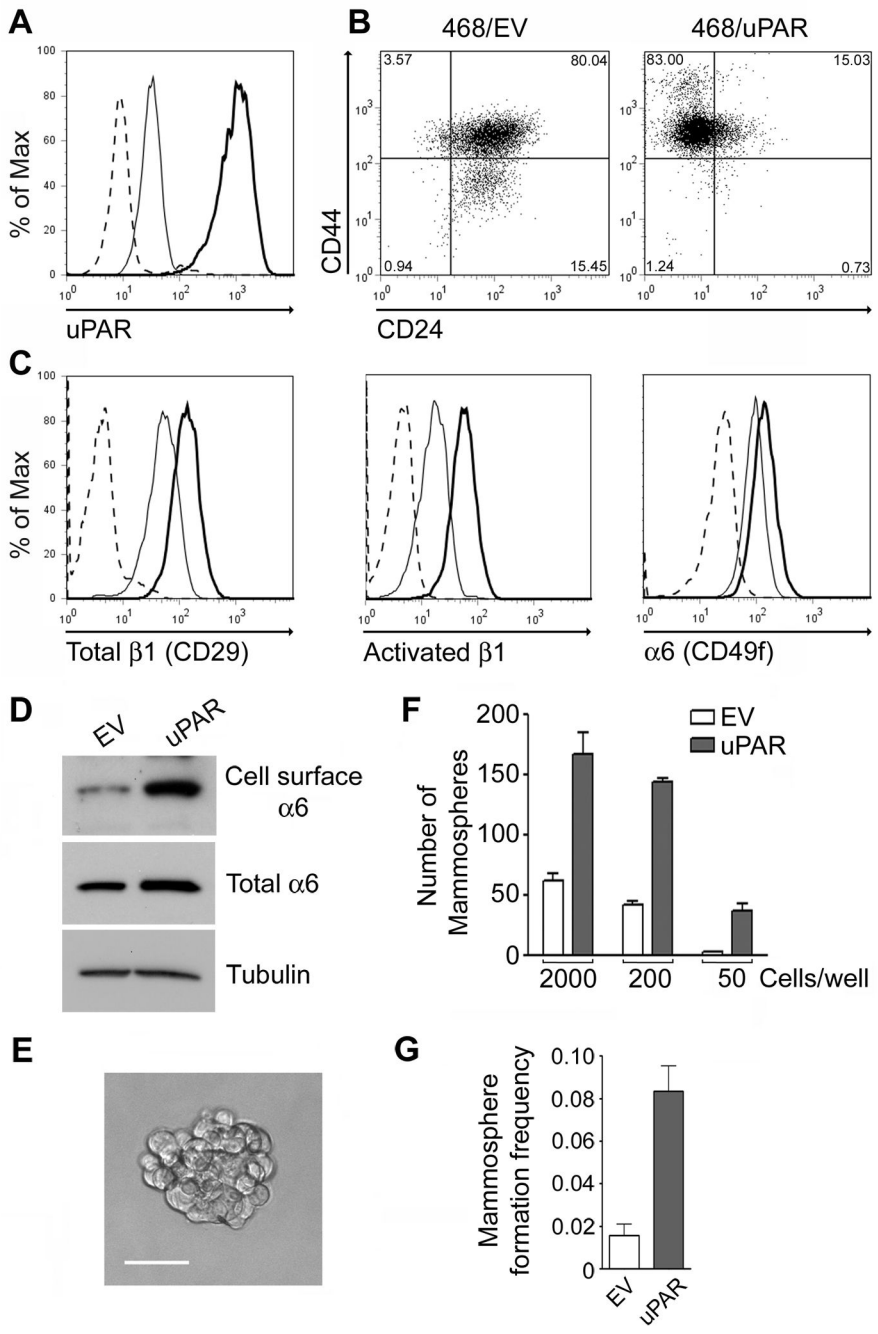

Figure 1.

uPAR over-expression in MDA-MB-468 cells induces CSC-like properties. *A*, Flow cytometry to detect uPAR in 468/uPAR (heavy curve) and 468/EV (light curve) cells. *B*, CD24 and CD44 were determined in 468/uPAR and 468/EV cells. Isotype-matched IgG controls are presented in Supplemental Figure 1A. *C*, Total β1/CD29, activated β1, and α6/CD49f were determined in 468/uPAR (heavy curve) and 468/EV (light curve) cells. The isotype-matched IgG is shown with a dashed line. *D*, α6 integrin and tubulin in affinity precipitates and whole-cell extracts from 468/EV and 468/uPAR cells were determined. *E*, Representative mammosphere formed by 468/uPAR cells (Bar, 50 μm). *F*, 468/uPAR and 468/EV cells were introduced into suspension culture at the indicated densities. Mammospheres were counted. The bar graph

shows one of three independent experiments, which generated similar results (mean ± SEM). *G*, Single-cell cultures were maintained for 7–10 days before determining the frequency of mammosphere formation (n=4, mean ± SEM).

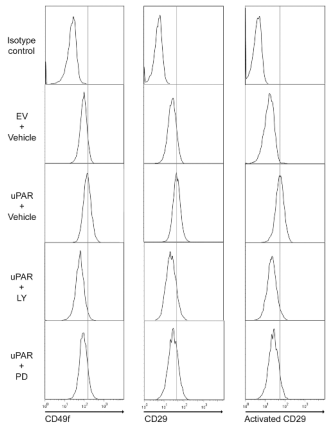

Figure 2.

Cell-surface integrin expression in 468/uPAR cells is inhibited by antagonizing PI3K or MEK. 468/EV and 468/uPAR cells were treated with LY294002 (10 μM), PD098059 (50 μM) or vehicle for 18 h. β1/CD29, activated β1, and α6/CD49f were determined by flow cytometry. The results are representative of three independent experiments.

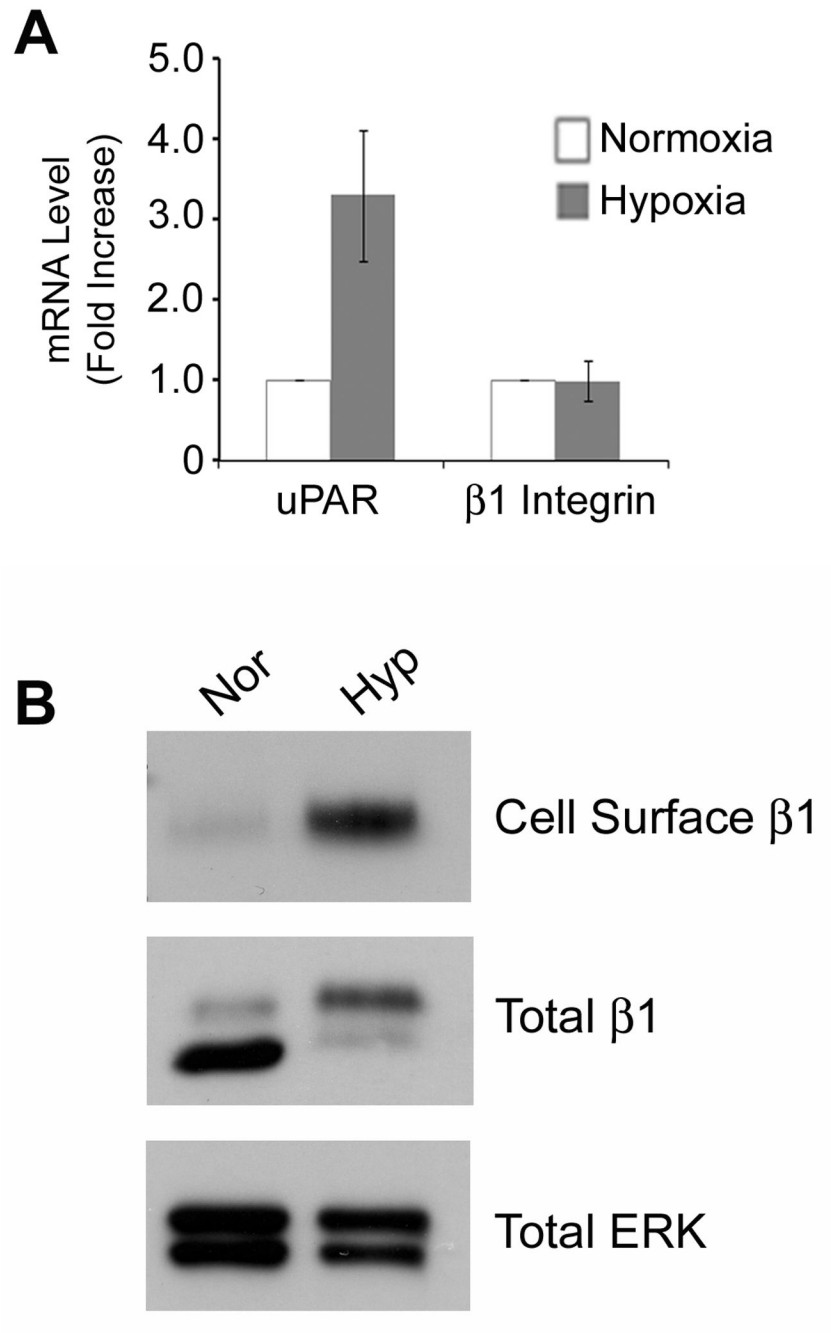

Figure 3.

Hypoxia increases the abundance of cell-surface β1 integrin in MDA-MB-468 cells. *A*, MDA-MB-468 cells were cultured in 21% O_2 (open bar) or 1.0% O_2 (closed bars) for 48 h. uPAR and β1 integrin mRNA were determined by qPCR and standardized against the levels in cells cultured in 21% O_2 (mean ± SEM; n = 3). *B*, MDA-MB-468 cells were cultured in 21% or 1.0% O_2 for 48 h. Affinity precipitates and whole cell-extracts were analyzed to detect β1 integrin and, as a control, total ERK/MAP kinase.

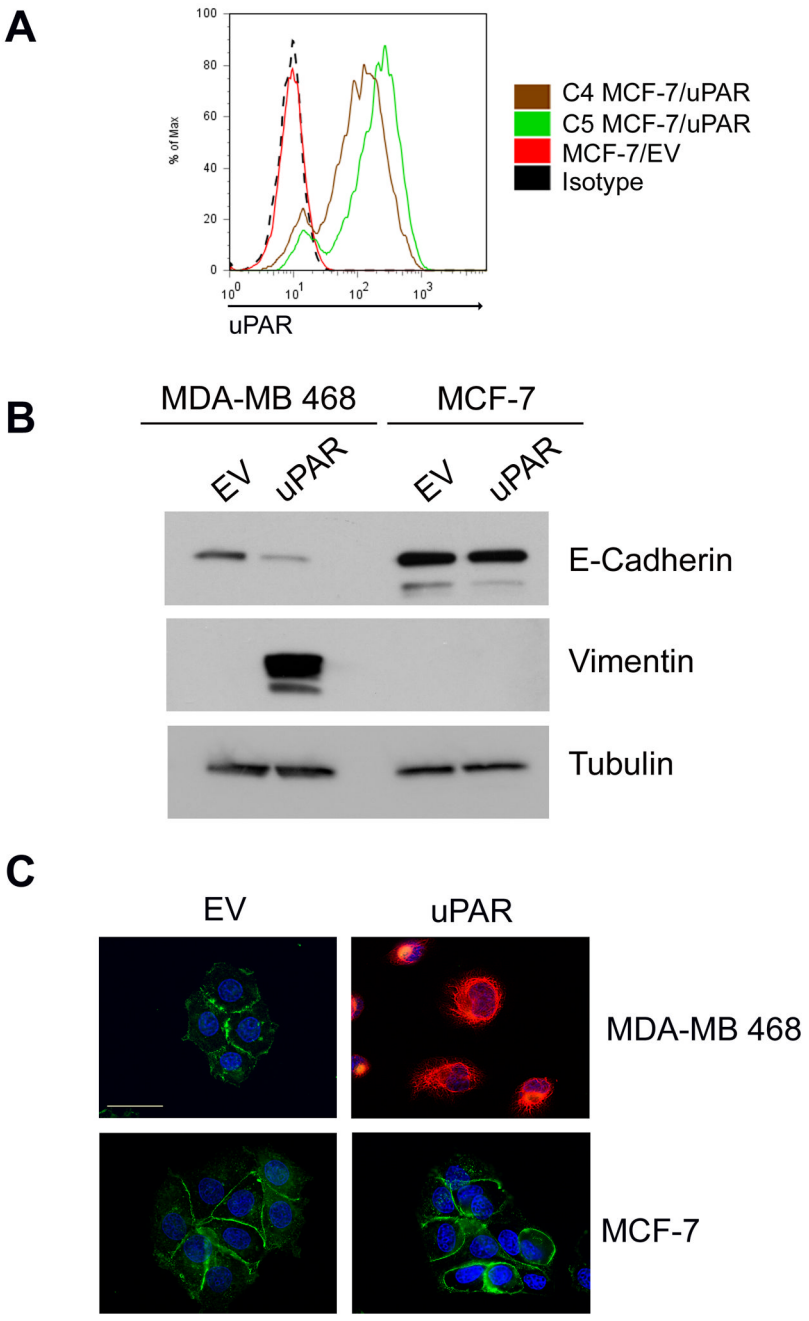

Figure 4.

uPAR over-expression does not induce EMT in MCF-7 cells. *A*, Flow cytometry to detect uPAR in C4 MCF-7/uPAR, C5 MCF-7/uPAR, and MCF-7/EV cells. *B*, Cell extracts from 468/EV, 468/uPAR, MCF-7/EV and C5 MCF-7/uPAR cells were subjected to immunoblot analysis to detect e-cadherin, vimentin and tubulin. *C*, 468/EV, 468/uPAR, MCF-7/EV and MCF-7/uPAR cells were immunostained to detect e-cadherin (green), vimentin (red), and DAPI (blue). The representative photomicrographs show all channels imaged simultaneously. Bar, 30 μm.

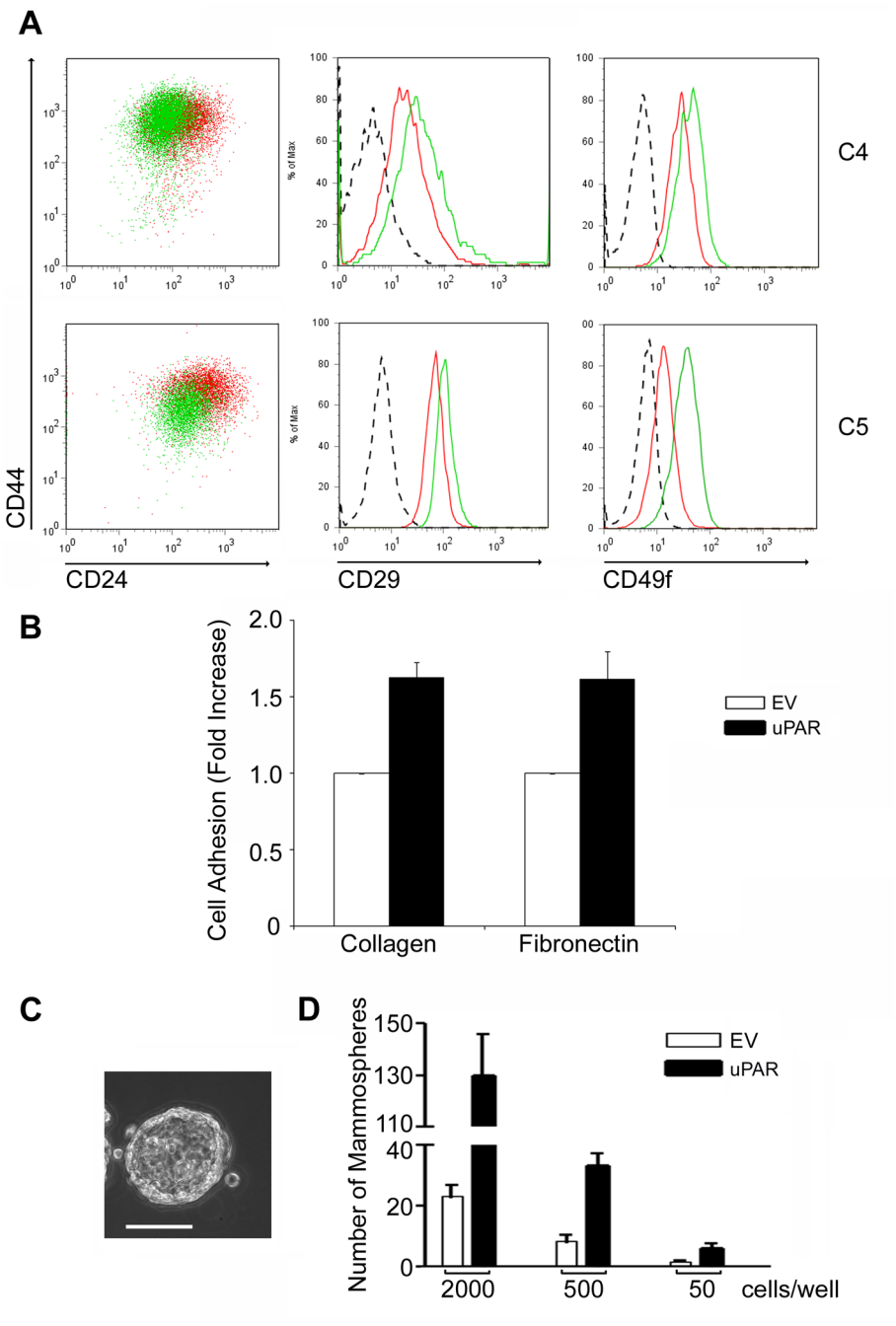

Figure 5.

uPAR over-expression induces CSC-like properties in MCF-7 cells. *A*, CD24, CD44, β1/CD29 and α6/CD49f were determined in MCF-7/EV cells, C4 MCF-7/uPAR cells, and C5 MCF-7/uPAR cells by flow cytometry (Red: MCF-7/EV, Green: MCF-7/uPAR, Dashed line: isotype control). The isotype control for CD24 and CD44 is shown in Supplemental Figure 1B. *B*, MCF-7/EV and C5 MCF-7/uPAR cells were seeded in collagen- or fibronectin-coated plates. Cell adhesion is expressed as the fold-increase relative to that observed with EV cells (mean ± SEM, n=3). *C*. Representative mammosphere formed by C5 MCF-7/uPAR cells (Bar, 100 μm). *D*. Mammosphere formation by C5 MCF-7/uPAR and MCF-7/EV cells was determined

after seeding wells with the indicated number of cells. The bar graph represents one of three independent experiments, which generated similar results (n=4 in each study, mean ± SEM).

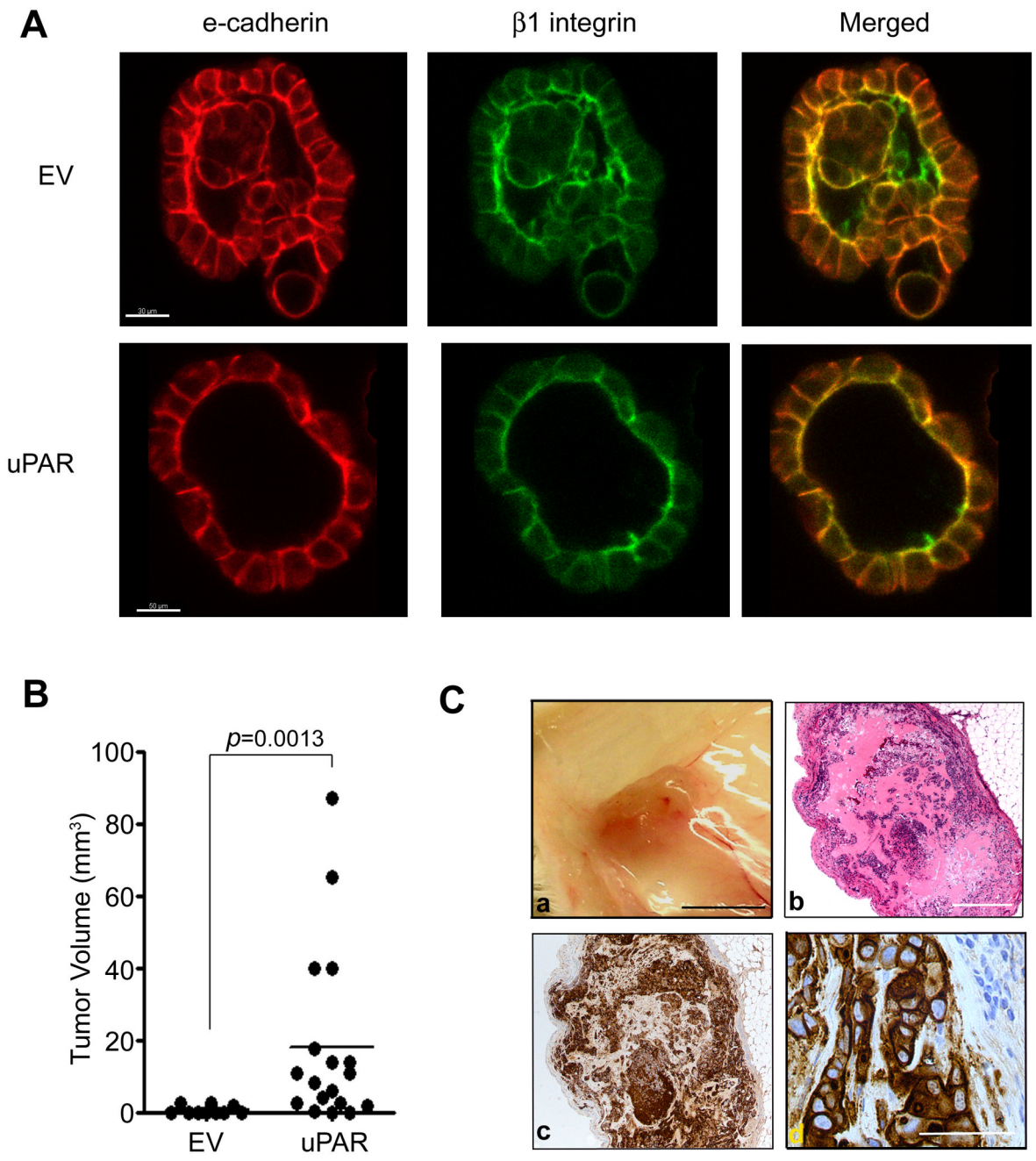

Figure 6.

MCF-7/uPAR cells form well-differentiated mammospheres and initiate tumor formation at an increased frequency *in vivo*. *A.* Mammospheres formed by MCF-7/EV and C5 MCF-7/uPAR cells were immunostained to detect e-cadherin (red) and β1 integrin (green). Single confocal optical sections (1 μm) are shown (Bar, 30 μm for MCF-7/EV cells and 50 μm for C5 MCF-7/uPAR cells). *B.* SCID mice were injected with C5 MCF-7/uPAR or MCF-7/EV cells. Tumor volume was determined after surgical resection (median, p=0.0013, Mann-Whitney rank sum test). *C.* Images of tumors formed by MCF-7/uPAR cells include: a) the gross tumor (Bar, 0.5 mm); b) microscopic section of a representative tumor (Bar, 500 μm); c) immunohistochemistry to detect human uPAR (magnification, 5×); d) higher magnification

image of immunohistochemistry to detect human uPAR. Notice blue-counterstained nuclei of non-malignant mouse cells infiltrating the tumor in the upper right-hand corner (magnification: 40×, Bar, μm).

Table 1

Frequency of tumor formation by 468/EV and 468/uPAR cells when injected into mammary fat pads in limiting dilution.

Number of Cells/ Injection	468/EV	468/uPAR	*P* value
1000	4/4	4/4	
100	4/4	4/4	
50	2/8	6/8	$p<0.05$

Statistical analysis = χ^2